DYNAMIC FIELD QUALITY OF LHC/SACLAY ARC QUADRUPOLE MAGNET PROTOTYPE

A. Devred, J. Belorgey, J. Deregel, B. Gallet, P. Genevey, F. Kircher, J.M. Rifflet, J.C. Sellier, and P. Védrine
CEA Saclay, DSM/DAPNIA/STCM, 91191 Gif-sur-Yvette Cedex, France
J. Billan – CERN, LHC/MMS, 1211 Genève 23, Switzerland
T. Ogitsu – KEK, National Laboratory for High Energy Physics, 1–1 Oho, Tsukuba-shi, Ibaraki-ken 305, Japan

ABSTRACT

As part of the magnet R&D program for the Large Hadron Collider (LHC), CEA Saclay has designed and built two 3-m-long, 56-mm-twin-aperture arc quadrupole magnet prototypes. Extensive field quality measurements were performed during the cold-test of the second prototype. A review of the field quality data as a function of ramp rate is presented. The observed field distorsions are explained in terms of inter-strand coupling currents arising from low and non-uniform resistances at the crossovers between the strands of the two-layer Rutherford-type cable. Last, the distribution of crossover resistances within the quadrupole magnet coil is determined.

INTRODUCTION

The field produced by superconducting particle accelerator magnets has three main components: 1) a component, B_t, resulting from the transport current, I, 2) a component, B_m, resulting from persistent magnetization currents arising in the superconducting filaments, and 3) a component, B_c, resulting from cable coupling currents. B_t only depends on the coil geometry and is expected to vary linearly as a function of I. B_m is dominated by the superconductor critical current density, which depends on temperature and magnetic field, and which decreases as a function of I. B_c only appears when the current is ramped and is expected to be independent of I and to vary linearly as a function of (dI/dt). In addition, magnetization of the surrounding iron yoke enhances each of the field components. The iron contribution is expected to follow the same dependence as the coil contributions, except at high transport currents, where saturation effects may occur.

In a previous paper,[1] we reviewed selected field quality data from a 3-m-long, 56-mm-twin-aperture quadrupole magnet prototype developed for the LHC arcs. The magnet, which relied on a two–layer, $\cos(2\theta)$ coil, wound from a Rutherford-type cable, reached its nominal gradient of 252 T/m at 15060 A with little training.[2,3] The geometric field errors, estimated from magnetic measurements at constant current and various axial positions along the magnet length, appeared to be quite small. The contributions from persistent magnetization currents, determined from measurements at a given axial position during the successive plateaus of a staircase current loop were consistent with predictions from standard theoretical models. Finally, a slight field-dependence of the magnetic permeability of the stainless steel collars used to constrain the magnet coil was held responsible for unexpected non-linear variations as a

function of I observed on the geometric field component. (For the LHC/Saclay quadrupole magnet, the iron saturation effects are negligible.)

In this paper, we complete our review by discussing magnetic measurement data taken at a given axial position while ramping the current up and down continuously at various ramp rates. Such data allow one to estimate the contributions from cable coupling currents. Large field distorsions as a function of ramp rate were observed on a number of dipole magnet prototypes developed for the Superconducting Super Collider (SSC).[4] Detailed analyses of the SSC magnet ramp rate sensitivity led to the elaboration of a model of cable interstrand coupling currents.[5,6] The same model is applied here to interpret the data from the LHC/Saclay quadrupole magnet prototype.

MULTIPOLE FIELD EXPANSION

In the quadrupole magnet straight section, the field can be considered as two dimensional and is conveniently represented by a multipole expansion

$$B_y + iB_x = \sum_{n=1}^{+\infty}(B_n + iA_n)\left(\frac{x+iy}{R_{ref}}\right)^{n-1} \quad , \quad (1)$$

where B_x and B_y are the x- and y- components of the field, B_n and A_n are the *normal* and *skew* $2n$-pole field coefficients, and R_{ref} is the reference radius. (For LHC magnets, $R_{ref} = 1$ cm). The symmetries of a $\cos(2\theta)$ conductor distribution are such that only the B_{4k+2} field coefficients, also called *allowed* multipole field coefficients, are expected to be non zero. Furthermore, it can be shown that, in first approximation, the persistent magnetization currents only affect the allowed multipole coefficients.

MEASURING DEVICE AND PROCEDURE

The multipole field coefficients are measured using a 700-mm-long rotating coil array.[1] The coils are connected to a voltage switching unit which allows the read-out of selected coil combinations and which includes several stages of amplifiers. The output voltage is sent to a voltage-to-frequency converter which integrates the signal between trigger pulses given by an angle encoder located at one end of the coil array. The fact that the current, hence the field, is varying during the measurement is corrected by recording the time of each trigger pulse and by considering a set of successive rotations. The data from the different rotations corresponding to a same angle interval are fitted as a function of time. The fits determined for the different angle intervals are then used to

interpolate the data at a number of selected times (one per rotation). Last, the interpolated data at each selected time are processed by mean of a discrete Fourier transform and converted into multipole field coefficients. The rotation period is 5 s.
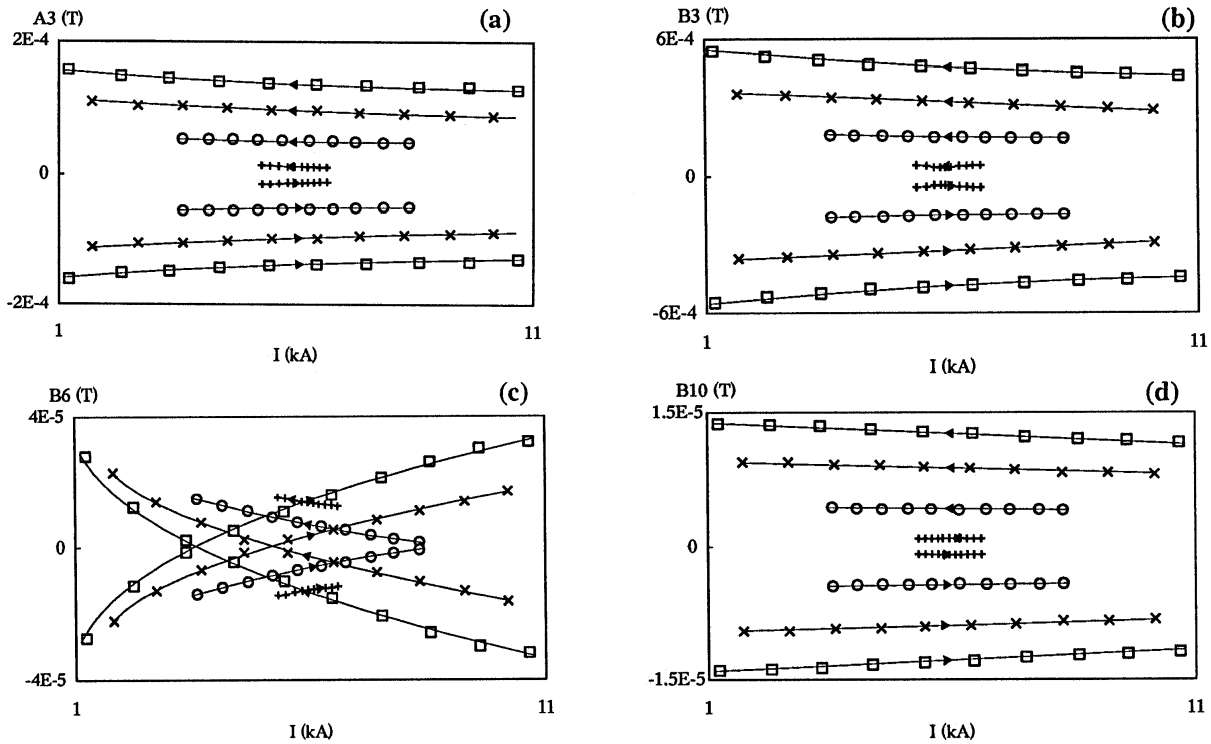
Figure 1. Rescaled multipole field coefficients as a function of current for a series of sawtooth ramps at increasing ramp rates (5 A/s (+), 20 A/s (o), 40 A/s (x), and 60 A/s (□)): a) skew sextupole field coefficient (A_3), b) normal sextupole field coefficient (B_3), c) normal dodecapole field coefficient (B_6), and d) normal 20-pole field coefficient (B_{10}). The field coefficients are in tesla.

MEASUREMENT RESULTS

Figures 1(a) through 1(d) display typical measurement results taken during series of sawtooth current ramps at increasing ramp rates. The coil array was located at the axial center of one aperture. For each ramp rate, the multipole field coefficients, $A_{n,r}$ and $B_{n,r}$, reported in the figures are rescaled in order to substract the geometric terms using

$$A_{n,r}(I) = A_n(I) - (A_{n,u} + A_{n,d})/2 \qquad (2a)$$

and

$$B_{n,r}(I) = B_n(I) - (B_{n,u} + B_{n,d})/2 \qquad (2b)$$

where $A_{n,u}$ and $B_{n,u}$ designate the multipole field coefficient values at I during the up-ramp and $A_{n,d}$ and $B_{n,d}$ designate the multipole field coefficient values at I during the down-ramp.

In a quadrupole magnet, the first multipole field coefficient expected to be affected by persistent magnetization currents is B_6. It appears in Figs. 1(a) and 1(b) that the re-scaled skew and normal sextupole field coefficients both exhibit sizable hystereses as a function of current, even at 5 A/s. It appears also that the

hystereses widths are roughly constant as a function of current, but increase quasi linearly as a function of ramp rate. Similar observations can be made for most un-allowed multipole field coefficients.

Turning now to Fig. 1(c), it appears that the rescaled B_6 describes hystereses whose widths vary as a function of current. Furthermore, at 5 A/s, the lower branch of the plot corresponds to the current up-ramp, while the upper branch corresponds to the current down-ramp. As the ramp rate is increased, the up-ramp branch moves upward while the down-ramp branch moves downward. The two branches cross each other a little below 8 kA at 20 A/s. The crossing current decreases to 4.2 kA at 40 A/s and 2.6 kA at 60 A/s, where the hysteresis is described almost entirely in a direction opposite to that observed at 5 A/s. In addition, it can be verified that, at a given current, the hysteresis width varies quasi linearly as a function of ramp rate. The behavior of the rescaled B_{10} shown in Fig. 1(d) resembles that of the sextupole field coefficients, but the amplitudes of the effects are smaller.

The data presented here exhibit the same features as the magnetic measurement data from the SSC dipole magnet prototypes mentioned in introduction.[4-6] The behaviors of the rescaled un-allowed multipole field coefficients are consistent with what can be expected from the effects of

cable coupling currents. Coupling currents also affect the allowed multipole coefficients. They appear to compete with the effects of persistent magnetization currents in the case of the rescaled B_6 but are largely predominant in the case of the rescaled B_{10}.
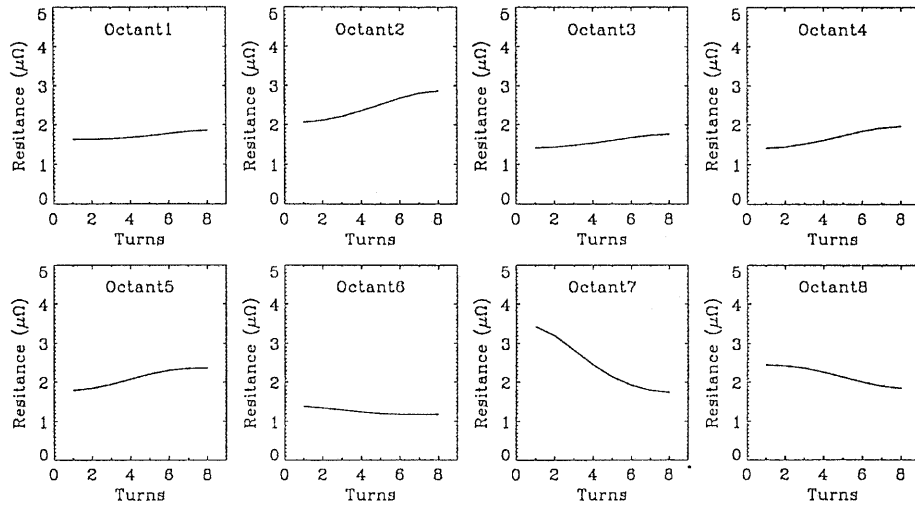
Figure 2. Estimated crossover resistance as a function of turn number in the various octants of one aperture of a LHC/Saclay arc quadrupole magnet prototype. The optimization process was carried out using magnetic measurement data as a function of ramp rate taken at the magnet axial center. The crossover resistances are in ohm.

DATA ANALYSIS

As for SSC dipole magnet prototypes, the dynamic field behavior of the LHC arc quadrupole magnet prototype seems to be dominated by cable interstrand coupling currents. The LHC prototype uses a flat, two-layer, slightly keystoned Rutherford-type cable with a radial width of 13.05 mm and a mid-thickness of 1.93 mm. It is made of 24 strands (strand diameter: 1.09 mm) which are coated with *staybrite* (a silver-tin coating). The cable pitch length is 100 mm.

During cabling, the strands are deformed heavily and large contact areas are created at the crossovers between the strands of the two layers. Furthermore, during and after magnet assembly, large pressures are applied perpendicularly to the cable which put the strands firmly in contact. If the contacts are good, the crossovers may provide low resistance paths for interstrand coupling currents to flow from one strand to another when the cable is subjected to a varying field.

Such a cable can be described by a network model where the strands are connected by resistances at each crossover points.[5] Representing every turn of a magnet coil by a network model, and knowing all the values of crossover resistances, it is then possible to determine the interstrand coupling current distribution and the resulting field distorsions. Conversely, having measured the field distorsions attributed to interstrand coupling currents, one can attempt, by an optimization process, to determine the crossover resistance distribution within the magnet coil.

Figure 2 presents the results of such an optimization. The followed process was identical to the one developed to interpret the SSC data and is described elsewhere.[6] It assumes that the crossover resistance is uniform within the coil outer-most layer and within every turn of the coil inner-most layer, but

that, for the inner layer, it can vary from turn to turn. The crossover resistance appears to vary from 1.2 $\mu\Omega$ to 3.2 $\mu\Omega$, with an average value of the order of 2 $\mu\Omega$. The distribution is more uniform than the ones determined for the SSC dipole magnet prototypes, but the average value is somewhat smaller. The strands used in SSC cables were not coated.

CONCLUSION

The observed dynamic field behavior of the LHC/Saclay quadrupole magnet prototype can be explained in terms of cable interstrand coupling currents, with a rather uniform distribution of low crossover resistances.

REFERENCES

[1] A. Devred, *et al.*, "Field Quality of LHC/Saclay Arc Quadrupole Magnet Prototype," Proc. 5th Eur. Part. Acc. Conf., pp. 2225-2227 (1996).
[2] J.M. Rifflet, *et al.*, "Cryogenic and Mechanical Measurements of the First Two LHC Lattice Quadrupole Prototypes," Proc. 4th Eur. Part. Acc. Conf., pp. 2265-2267 (1994).
[3] P. Genevey, *et al.*, "Cryogenic Tests of the First Two LHC Quadrupole Prototypes, IEEE Trans. Appl. Super., Vol. 5(2), pp. 202-205 (1995).
[4] T. Ogitsu, *et al.*, "Influence of Cable Eddy Currents on Magnetic Field Harmonics," KEK–Proc. 92–14, pp. 23-27 (1992)
[5] T. Ogitsu and A. Devred, "Ramp Rate Sensitivity of SSC Magnets," *Frontiers of Accelerator Magnet Technology*, S.I. Kurokawa, M. Month, S. Turner, eds., World Scientific, pp. 184-308 (1996).
[6] T. Ogitsu, *et al.*, "Influence of Inter-strand Coupling Currents on Field Quality of Superconducting Accelerator Magnets," submitted to Particle Accelerators.